Am J Transl Res 2019;11(7):4063-4076
www.ajtr.org /ISSN:1943-8141/AJTR0092648

Original Article

Clinical improvement and enhanced collateral vessel growth after xenogenic monocyte transplantation

Martin Wagner[1*], Adrian Mahlmann[2*], Elisabeth Deindl[3], Werner Zuschratter[4], Monika Riek-Burchardt[5], Sawa Kostin[6], Blerim Luani[1], Claudia Baer[1], Akram Youssef[7], Joerg Herold[1,8]

[1]Department of Cardiology and Angiology, Otto-von-Guericke University of Magdeburg, Magdeburg, Germany; [2]Department of Medicine - Section Angiology, Carl Gustav Carus University of Dresden, Germany; [3]Department of Experimental Medicine, Walter Brendel Centre, Munich, Germany; [4]Leibniz Institute for Neurobiology, Magdeburg, Germany; [5]Institute of Molecular and Clinical Immunology, Otto von Guericke University of Magdeburg, Magdeburg, Germany; [6]Max-Planck-Institute, Bad Nauheim, Germany; [7]Department for Internal Medicine and Cardiology, University of Dresden, Germany; [8]Department of Vascular Medicine, Klinikum Darmstadt GmbH, Max-Ratschow Clinic for Angiology, Darmstadt, Germany. [*]Equal contributors.

Received February 16, 2019; Accepted June 7, 2019; Epub July 15, 2019; Published July 30, 2019

Abstract: *Background*: Monocytes (Mo) are the most important mediators in arteriogenesis. Previous results from our group demonstrated the great potential of allogenic Mo transplantation for improving collateral vessel growth, which appeared to be due to a considerable host vs. graft reaction. To prove this hypothesis and introduce this new method in clinical practice, we performed transplantation of human Mo (HuMo) in a mouse model. *Methods and results*: We ligated the femoral artery of BALB/c mice and transplanted Mo via the tail vein. Perfusion was measured by laser Doppler perfusion imaging (LDPI). We also performed clinical scoring based on behavior, wound healing, signs of inflammation and mobility of the ligated extremity. Finally, arteriogenesis and angiogenesis were examined histologically and by quantitative RT-PCR of the hind limb musculature. LDPI increased within one week after ligation when HuMo were transplanted and increased further up to day 21 (0.63±0.12 (n=12) in HuMo vs. 0.50±0.12 (n=17) in the control group (P<0.01)). A histological evaluation showed significantly more collateral arteries within the adductor muscles after HuMo transplantation. The promotion of collateral vessel growth after HuMo transplantation resulted in better clinical scores (0.33±0.26 (n=12) vs. 3.3 (n=9), SEM; P<0.01). *Conclusions*: Transplantation of HuMo improves collateral vessel growth and clinical outcomes in mice. These results verify our hypothesis that controlled triggering of the inflammatory mechanism resulted in collateral vessel growth by a local host vs. a graft reaction in the ischemic hind limbs and could represent a further step in the development of a clinical strategy for promoting arteriogenesis.

Keywords: Arteriogenesis, angiogenesis, monocyte, cell transplantation, innate and adaptive immune system, inflammation

Introduction

The endogenous response of the body to a progressive vascular disease with consecutive luminal narrowing (e.g., peripheral artery disease or coronary artery disease) is the active remodeling and growth of pre-existing arterioles towards larger functional collateral arteries, which is a process termed arteriogenesis [1]. Indeed, an association between collateral blood flow, myocardial viability and reduced long-term mortality has been demonstrated in patients with coronary heart disease [2-4]. However, only approximately one-third of the maximal conductance of a normal artery is restored by endogenous collateral artery growth [5]. Hence, therapeutic stimulation of arteriogenesis represents an appealing concept, especially considering that 20% of patients with vascular disease are not suitable for current treatments, such as percutaneous interventions or surgical bypass grafts [6]. The pathogenesis of collateral growth (arteriogenesis) has been linked to both the innate and adaptive immune systems. While therapeutic approaches for the augmentation of arteriogenesis have focused on innate

immunity, exploiting both innate and adaptive immune responses has not been widely examined. Collateral vessel growth is strongly driven by local inflammation [7]. This inflammatory response includes endothelial activation and the local recruitment of leukocytes, mainly monocytes (Mo) [8]. Mo mature to macrophages and create a highly arteriogenic environment by secreting multiple growth factors that induce the remodeling of arterioles into functional collateral arteries [9-11].

Our group has focused on the idea that increasing local inflammation may represent the best stimulus for arteriogenesis. We have exploited the homing of Mo to areas of collateral growth for cell transplantation studies [12]. Intriguingly, transplantation of allogeneic Mo resulted in the strongest arteriogenic response, implying that, indeed, targeting both the innate and adaptive immune systems may be the most efficient way to clinically augment collateralization [12-14]. We demonstrated that autologous Mo are attractive vehicles for augmentation of arteriogenesis via immunomodulation, which has been previously demonstrated in rabbits and mice [12-15]. For further clinical implementation, we carried out this study to investigate the potential of human monocytes (HuMo) in a mouse model. The aim of this study was to systemically transplant HuMo into a mouse model of hind limb ischemia and then visualize their homing and analyze their therapeutic potential. Intravital microscopy was used for in vivo imaging and to evaluate the transmigration of exogenous HuMo to areas of collateralization. In addition to laser Doppler imagining of hind limb reperfusion after ligation of the femoral artery, we evaluated clinical scores to investigate the clinical effect of the transplantation strategy.

These techniques were subsequently confirmed by histological analyses of muscle. We analyzed collateral vessel growth within the upper limb (adductor muscle) and angiogenesis within the lower limb (gastrocnemius muscle). qPCR of muscle tissue was performed to detect possible mechanisms of vessel growth. Systemic immunological reactions and/or inflammation were investigated via a multiplex cytokine assay of peripheral blood samples of mice across various time points, including before and up to 14 days after transplantation.

This study was developed to shed light on understanding the complex and potent capacity of Mo transplantation for augmentation of arteriogenesis in peripheral artery disease.

These observations will support the elaboration of clinically applicable immunotherapeutic approaches [14, 16].

As Mo isolation from humans and subsequent *ex vivo* engineering are both easy to perform and safe, strategies utilizing HuMo are highly attractive for translation to clinical therapies.

Materials and methods

Monocyte isolation

For monocyte isolation and characterization, we used a previously published protocol by our group [13-18] and protocols from [19, 20]. We resuspended the cells with cell culture medium (M199 (PAA Laboratories, Pasching, Austria) + 10% fetal calf serum (FCS) (Sigma Aldrich, Hamburg, Germany) + 1% penicillin/streptomycin (Sigma Aldrich, Hamburg, Germany) and seeded the cells on 6-well ultra-low attachment plates (Corning Incorporated, NY, USA). We added 8 ng/ml IFN-γ (Thermo Fisher, Waltham, Massachusetts, USA) to the cell suspension and incubated the cells for one day at 37°C and 5% CO_2.

Mouse femoral artery ligation model

Eight- to twelve-week-old BALB/c mice were anaesthetized with 100 mg/kg body weight ketamine hydrochloride (Ketanest, Pfizer, Berlin, Germany) and 2 mg/kg body weight xylazine hydrochloride (Rompun, Bayer, Leverkusen, Germany). The femoral artery was occluded by double ligation with 6-0 silk sutures (Ethicon, Norderstedt, Germany) distal to the origin of the deep femoral artery and proximal to the *A. epigastrica superficialis* [13, 21]. All procedures involving experimental animals were approved by the local government animal care committee (AZ:42502-2-1333) and complied with the Guide for the Care and Use of Laboratory Animals (NIH publication No. 86-23, revised 1985).

Monocyte transplantation

One day after femoral ligation, 2.5×10^6 HuMo resuspended in 150 µl saline were injected via the tail vein. Afterwards, the animal was monitored for 30 min for systemic side effects [17].

The mouse was placed in its cage after fully recovering.

Laser doppler perfusion imaging (LDPI)

LDPI was used to measure serial blood flow before and after ligation of the left femoral artery and for three weeks postoperatively. The animals were placed for 5 min on a 37°C heating plate (Föhr Instruments, Seeheim-Ober, Germany) to avoid vasoconstriction by anesthetic heat loss. To calculate hind limb perfusion, the mean pixel intensity of both legs was determined, and a "perfusion index" (ligated side/unligated side) was used for quantification [14, 22].

Immunohistochemistry and morphometrical analysis

Tissue samples of adductor and gastrocnemius muscle from both hind limb muscles were snap-frozen in methyl butane 1, 3 and 21 days after ligation and stored at -80°C until use [23]. Cryosections (5-7-µm thick) were prepared with a Leica CM Cryostat (Leica Biosystems, Nussloch, Germany), fixed and permeabilized in ice-cold acetone, and blocked with a serum-free protein block (Dako, Hamburg, Germany) for 20 minutes. They were then incubated with rabbit anti-CD31 (Abcam, Cambridge, UK) for 1 h at room temperature, followed by the appropriate cross-absorbed secondary antibody conjugated to Cy3 fluorochrome (Jackson ImmunoResearch Suffolk, UK). An FITC-conjugated mouse anti-SMC-α-actin antibody (Sigma Aldrich, Hamburg, Germany) was included as a counterstain, followed by nuclear counterstaining with DAPI. Only vessels with a media-to-lumen-ratio typical for arteries were counted, and their diameters were determined. Sections were analyzed using an Axiovert 200 m (Carl Zeiss, Jena, Germany) equipped with appropriate filter sets and an AxioCam MRm (Carl Zeiss, Jena, Germany). Images of the sections were acquired using overlapping image acquisition and then stitching, and the images were then quantified by image segmentation and a particle analysis using ImageJ (https://imagej.nih.gov/ij/docs/faqs.html). For confocal microscopy, 10-µm-thick cryosections were fixed in 4% (wt/vol) paraformaldehyde and incubated with a rat antibody against the mouse CD68 antigen (Serotec, Puchheim, Germany). Sections were then incubated with biotinylated secondary donkey anti-rat antiserum (Dianova, Hamburg, Germany) and Cy2-Streptavidin (Rockland, USA). After repeated washes with PBS, sections were incubated with anti-SMC-α-actin directly labeled with Cy3 (Sigma Aldrich, Hamburg, Germany). F-actin was visualized with phalloidin conjugated with Alexa 633 (Molecular Probes, Thermo Fisher Scientific, USA). Finally, nuclei were stained with DAPI. The sections were examined by laser scanning confocal microscopy (Leica TCS5), which allows 4-channel concomitant scanning. Ten confocal optical sections were taken through the depth of the tissue samples at 0.5-µm intervals using a Leica Planapo 63/1.4 objective. Three-dimensional reconstruction was performed using Imaris 7.2 multichannel image processing software (Bitplane, Zurich, Switzerland).

Cell staining with DiO for IVM

Isolated HuMo were resuspended in serum-free culture medium (M199 (PAA Laboratories, Pasching, Austria) + 1% penicillin/streptomycin (Sigma Aldrich, Hamburg, Germany) overnight on 6-well ultra-low attachment plates (Corning Incorporated, NY, USA) at a density of 1×10^6 cells per ml. The cells were than labeled with 5 µM DiO (Life Technologies, Darmstadt, Deutschland) for 20 min at 37°C. Subsequently, culture medium was added and the cells were centrifuged at 300 × g for 5 min. The supernatant was dislodged, and resuspended cells were transplanted into the tail vein of mice for systemic administration [17].

Fluorescein-BSA lysotracker

To demonstrate that soluble tracking proteins from the cell culture medium are phagocytosed and accumulate, fluorescein-labeled BSA (Sigma Aldrich, Hamburg, Germany) was used. Bovine serum albumin (BSA) (GE Healthcare, Freiburg, Germany) was solved in 10 mg/ml in a 0.1 M $NaHCO_3$ buffer (pH 8.3) (PanReac Applichem, Darmstadt, Germany) and subsequently coupled with fluorescein by adding a carboxyfluorescein succinimidyl ester (CFSE) solution (Sigma Aldrich, Hamburg, Germany) at a final concentration of 1 mM. After 1 h, fluorescein-BSA was purified from residual CFSE by twofold dialysis. Purified fluorescein-BSA was added to isolated HuMo at a concentration of 100 µg/ml and incubated overnight. After washing three times with cell culture medium,

Table 1. Criteria and quantification of the clinical evaluation outcomes of the mice

Criteria of clinic score	Points
Wound healing	0-inconspicuous
	1-consp
Mobility	0-inconspicuous
	1-slight handicap
	2-mean handicap
	3-immobility
Skin of the ligated leg	0-inconspicuous
	1-slight redness
	2-livid discoloration
	3-Gangrene
Behaviour	0-inconspicuous
	1-conspicuous

Morphological, clinical and behavioral parameters and weight loss were analyzed. Lower scores represent better clinical outcomes with less impairment.

the Mo were counterstained with Hoechst 33342 and LysoTrackerRed DND-99 (Thermo Fisher Scientific, Schwerte, Germany). Subsequent z-Stack acquisition with an Axiovert 200 m equipped with an Apotome was used to localize fluorescein-BSA on the subcellular level.

Intra vital microscopy for visualizing the homing of HuMo

Live imaging of HuMo homing to sites of arteriogenesis *in vivo* was demonstrated by intravital microscopy (IVM), which is a minimally invasive optical imaging technique that offers high-resolution, deep tissue penetration and video capturing. By using this innovative and unique method we were able to examine the kinetics of monocyte homing *in vivo* and the endogenous development of collateral arteries within the hind limbs of mice after ligature of the femoral artery. The morphology of the collateral vessels in the adductor muscle was determined by live cell imaging, and blood flow was visualized within the growing arteries. For *in vivo* experiments, mice were anesthetized intraperitoneally and placed on a heating plate (37°C). The leg was then fixed between two adjustable stamps, and care was taken to keep the region of interest moist. A cover glass was positioned on top of the stamps and adjusted before imaging was begun. A Zeiss LSM 710 NLO (Carl Zeiss Microscopy, Goettingen, Germany) with a 20 × water immersion lens (NA 1.0) or a Leica SP 5 microscope (Leica Microsystems, Wetzlar, Germany), with a 10 × dry lens (NA 0.4) were used in either two photon or single photon confocal mode, respectively.

Clinical scoring

For clinical evaluation of the cell therapy and the augmentation of arteriogenesis, we developed a clinical score to evaluate and analyze the revascularization and outcomes of the animals. Morphology, clinical parameters, behavior, and weight loss were analyzed. Lower scores represented better clinical outcomes with less impairment (**Table 1**).

RNA isolation and qRT-PCR

Total RNA was isolated from tissue according to the method of Chomczynski and Sacchi [24]. Residual genomic DNA was removed using an RNase-Free DNase Kit (Promega, Mannheim, Germany). One microgram RNA was reverse transcribed into cDNA with random nonamers (Roche, Mannheim, Germany) and a 1st Strand cDNA Synthesis Kit for RT-PCR (Roche). qRT-PCR was performed using a Light Cycler 1.5 (StepOnePlus Applied Biosystems, Life Technologies, Darmstadt, Germany) and a SSYBR Green I Kit (Power Up SyberGreen Master Mix, ThermoFisher Scientific, Darmstadt, Germany) according to the manufacturer's protocol with 1 µl of the 1:5 diluted cDNA and 0.5 µM of each primer per reaction. The following primers were used: 18S rRNA forward 5'-GGACAGGATTGACAGATTGATAG-3', reverse 5'-CTCGTTCGTTATCGGAATTAAC-3'; monocyte chemoattractant protein 1 (MCP-1) forward 5'-CTCAAGAGAGAGGTCTGTGCTG-3', reverse 5'-GTAGTGGATGCATTAGCTTCAG-3'; proliferating cell nuclear antigen k-67 (ki67) forward 5'-GAGTGAGGGAATGCCTATG-3', reverse 5'-GCTGTGAGTGCCAAGAGAC-3'. At least two independent qRT-PCR reactions were performed on each template using following protocol: initial denaturation step at 95°C for 10 min followed by 40 cycles of denaturation at 95°C for 15 s, annealing at 64°C for 18 S rRNA, 62°C for MCP-1, 58°C for ki67, for 1 min each, and extension at 72°C for 15 s. To ensure specific amplification, agarose gels and melt curve analyses were performed. The ΔCt method was used to quantify the data, and the results were normalized to the expression levels of 18 S rRNA.

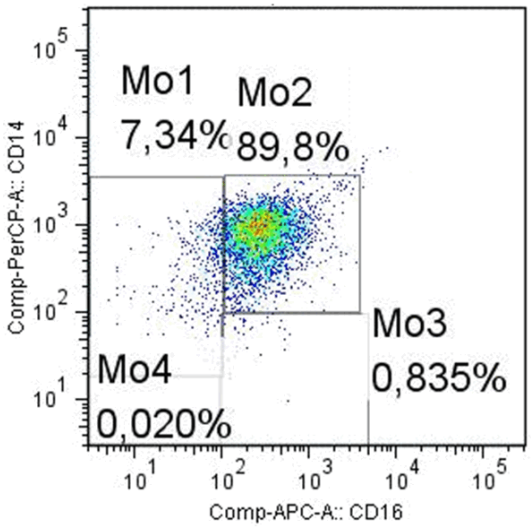

Figure 1. FACS analysis of transplanted HuMo: Exemplary illustration of INF-α-stimulated human monocyte subsets based on a typical distribution of events in a CD14 CD16 staining protocol. Subsets: classical monocytes (Mo1) $CD14^{++}CD16^{-}$, proinflammatory monocytes (Mo2) $CD14^{++}CD16^{+}$, non-classical monocytes (Mo3) $CD14^{+}CD16^{+}$ and (Mo4) $CD14^{-}CD16^{-}$.

Cytokine quantification by Luminex technology

Cytokine, chemokine and growth factor levels in mouse serum were quantified at different time points (blood sample time line: before ligation and at 8 h, 24 h, 72 h, 7 days, 14 days and 21 days after ligation). Serum was stored after a spin-down procedure at -80°C, and mice were i.p. injected with 250 µl saline after each blood withdrawal. The cytokine concentrations of IL-1α, IL-1ß, IL-2, IL-3, IL-4, IL-5, IL-6, IL-9, IL-10, IL-12 (p40), IL-12 (p70), IL-13, IL-17, eotaxin, G-CSF, GM-CSF, IFN-γ, KC, MCP-1 (MCAF), MIP-1α, MIP-1ß, RANTES and TNF-α were determined using a multiplex pro-mouse cytokine 23-plex panel and a cytokine reagent kit (Bio-Rad Laboratories, USA) as previously described [25]. Samples were analyzed in triplet and standards in duplicate using a Luminex-100 instrument with Bio-Plex Manager 4.1 software (Bio-Rad Laboratories, Munich, Germany) [26].

Statistics

Statistical analysis was carried out using SAS® software, version 9.2 (SAS Institute Inc., Cary, NC, USA) and SPSS 24 (IBM, Germany). The analyzed parameters are summarized as the mean ± SD and arithmetic average ± standard error of the mean for the results of the clinical score. The whiskers in the bar charts represent standard errors. In the experiments, the main effect (group) and the time effect (after ligation) for developing from pre to 21 days were of special interest. To analyze these effects we performed a two factorial ANOVA with cross effects using the GLM procedure in SAS®. In case of a significant global test, Tukey's test was used as a post hoc test for pairwise group comparisons. The significance levels were determined using the adjusted F-Test by Huynh-Feldt. *P*-values were used to indicate significant differences among the factors in the ANOVA. All statistical decisions were two-tailed with a critical probability of α=5% without α-adjustment except for Tukey's test for pairwise group comparisons. For all biochemical data, a one way ANOVA followed by the Bonferroni post hoc test was used. A p value of <0.05 was considered significant.

Results

Isolation

Before each cell transplantation, we conducted a FACS-Analysis to measure the number of Mo within each cell preparation and to calculate the number of cells that had to be injected. A representative FACS-Analysis for cell isolation is shown in **Figure 1**.

Main groups of Mo were differentiated. Classical Mo are represented by Mo1. The group of non-classical Mo is represented by Mo3. Most of our Mo are $CD16^{++}/CD14^{++}$ (Mo 2, 89.8%) which are consistent with intermediate Mo. This cell fraction is used for calculating the number of HuMo that had to be injected.

Fluorescein-BSA lyso tracker uptake experiments

Soluble proteins from the cell culture medium were phagocytosed and localized in lysosomes. As demonstrated, the fluorescein-labeled BSA accumulated in the lysosomes of treated HuMo (**Figure 2**).

LDPI

LDPI showed a decrease in the perfusion index (PI) from 0.99±0.09 preoperatively to 0.19±

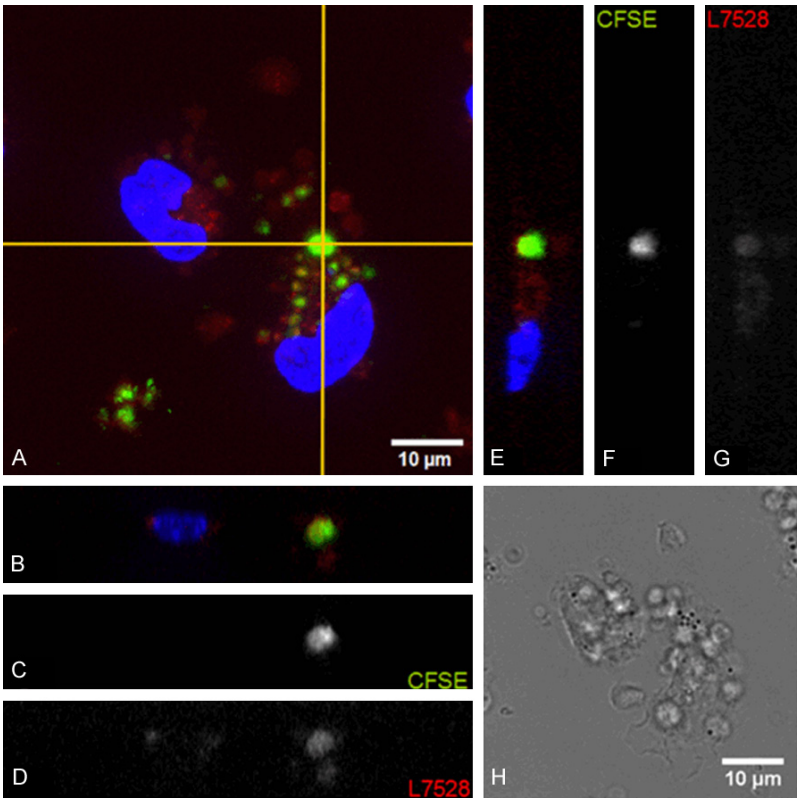

Figure 2. Fluorescence microscopy of two monocytes at 63x magnification. The kidney-shaped cell nuclei (blue, Hoechst 33342) of two monocytes with the surrounding cytoplasmic space are shown. The processed CFSE-BSA (green) (A) is located in the cytoplasm and lysosomes (red). (A) shows the maximum intensity projection of an acquired z-stack from two Mo. Nuclei are shown in blue, fluorescein-BSA in green and lysosomes stained by LysoTracker accumulation in red. The projections of the ontological planes (B-G), which are shown in green in (A), demonstrate the subcellular localization of BSA within lysosomes, thus implying a subsequent MHC antigen presentation of BSA. For a better overview and allocation of structures, a transmitted light image was acquired (H).

0.04 post-ligation in all groups. LDPI showed a marginal increase in the PI after HuMo transplantation (0.39±0.10 HuMo PI vs. 0.34±0.13 saline PI; n.s.) one week after ligature. On day 14, the PI was 0.54±0.06 in HuMo vs. 0.45±0.13 in the saline control (*P<0.05). The difference in PI between the HuMo and control cases increased until day 21 (HuMo PI 0.63±0.12; vs. saline PI 0.5±0.12; (n=17); **P<0.01) (**Figure 3**).

Clinical score (CS)

Prior to ligation, the condition of all animals was normal, and no points were assigned for any loss of function at baseline. The same scores were observed immediately after ligation (CS of 6 points for both groups). Greater recovery was observed in the HuMo-transplanted group on day 7 (3.2±0.64 saline vs. 2.17±0.21 HuMo; (SEM)). Following day 7, no further improvement in clinical outcome was observed in the control group. The clinical outcome of the HuMo transplantation group improved after transplantation, whereas on day 14, the CS of the control group had further decreased to 4.0±0.69 (SEM). The mice of the transplantation group also exhibited better clinical conditions on day 14 and the CS had decreased from 2.17±0.21 on day 7 to 1.25±0.29 (SEM) on day 14 (**P<0.01). No severe gangrene was detected in this group. On day 21, the CS of the HuMo group reached 0.33±0.26 (SEM), representing nearly the initial baseline value as assessed before the operation. In contrast, the saline group had a CS of 3.33±0.76 (SEM) (**P<0.01), which indicated a reduced clinical outcome (**Figure 4**).

Histology

The number of collateral arteries (ca) within the ligated leg increased when HuMo were transplanted (9.33±2.31 collateral arteries in the HuMo group (n=12) vs. 6.33±1.5 collateral arteries in the saline group (n=9), **P<0.01) (**Figure 5A**). This result was congruent with the LDPI results and the CS grades. The increasing number of collaterals resulted in better perfusion of the hind limbs and better clinical conditions of the animals. In addition to counting the collaterals, we also evaluated differences in the vessel diameter of the collaterals of both groups to draw conclusions about the quality of the collaterals. However, there were no differences between the HuMo and control saline groups (24.4 HuMo (n=6) vs. 26.67 saline (n=9), P>0.05, n.s.).

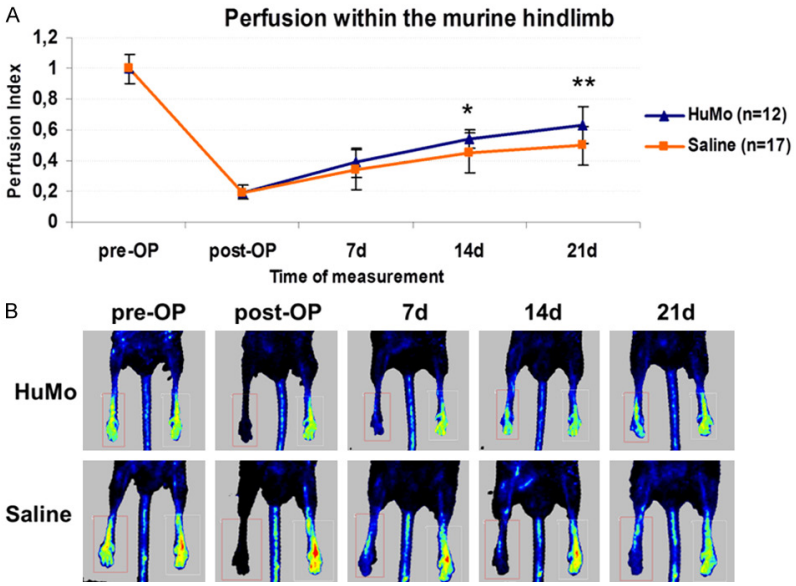

Figure 3. Comparison of hind limb perfusion over 21 days. LDPI measurements show a significant difference in perfusion after 14 days (*P<0.05), which increased after 21 days (**P<0.01) (A). Representative images of LDPI measurements illustrate the effect of augmentation of collateral vessel growth after monocyte transplantation (B).

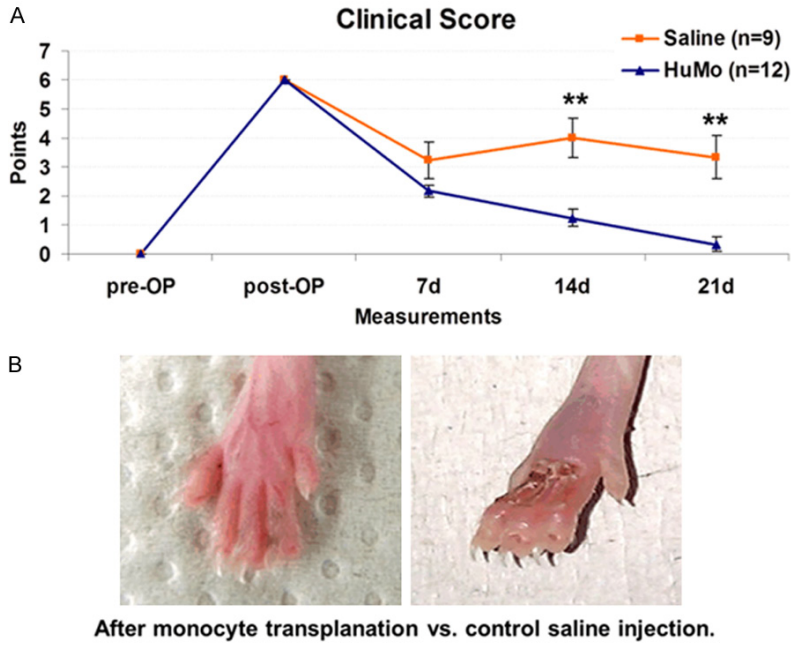

Figure 4. A. Clinical outcome of the animals evaluated based on the clinical score over 21 days. B. Representative pictures show the good clinical status of the mice after monocyte transplantation (left picture) and severe gangrene in control animals (right picture) after 21 days.

The increasing number of collateral arteries within the adductor muscle resulted in decreased ischemia in the lower limb. The number of CD31-positive capillaries within the gastrocnemius muscle 21 days after ligation of the femoral artery was 652±121 capillaries/mm^2 in the HuMo group (n=12) vs. 1001±305 capillaries/mm^2 in the saline group (n=9) (**P<0.01) (**Figure 5B**), and **Figure 5C** shows these results. In summary, HuMo augment the development of collaterals, thereby reducing capillary sprouting by positively influencing reperfusion.

Homing based on intravital microscopy (IVM)

Using IVM, we were able to capture multi-color videos of living cells. Ex vivo DiO-labeled HuMo (green) were visualized in vivo in areas of collateralization. The time course of HuMo was assessed by first visualizing HuMo within the vessel lumen (**Figure 6A**) and then after transmigration of HuMo within the perivascular space (sees previous publications [15]). Our data demonstrate that IVM is a potent tool for the visualization of collateral arteries in small animal models.

Immune histological verification of homing of transplanted monocytes

Histological evaluation of the IVM results and visualization of transplanted HuMo were performed to follow the route of endogenous mouse Mo after their transplantation, and the results supported our hypothesis that a mild local host vs. graft reaction can be used as a therapeutic tool for enhancing the inflammatory por-

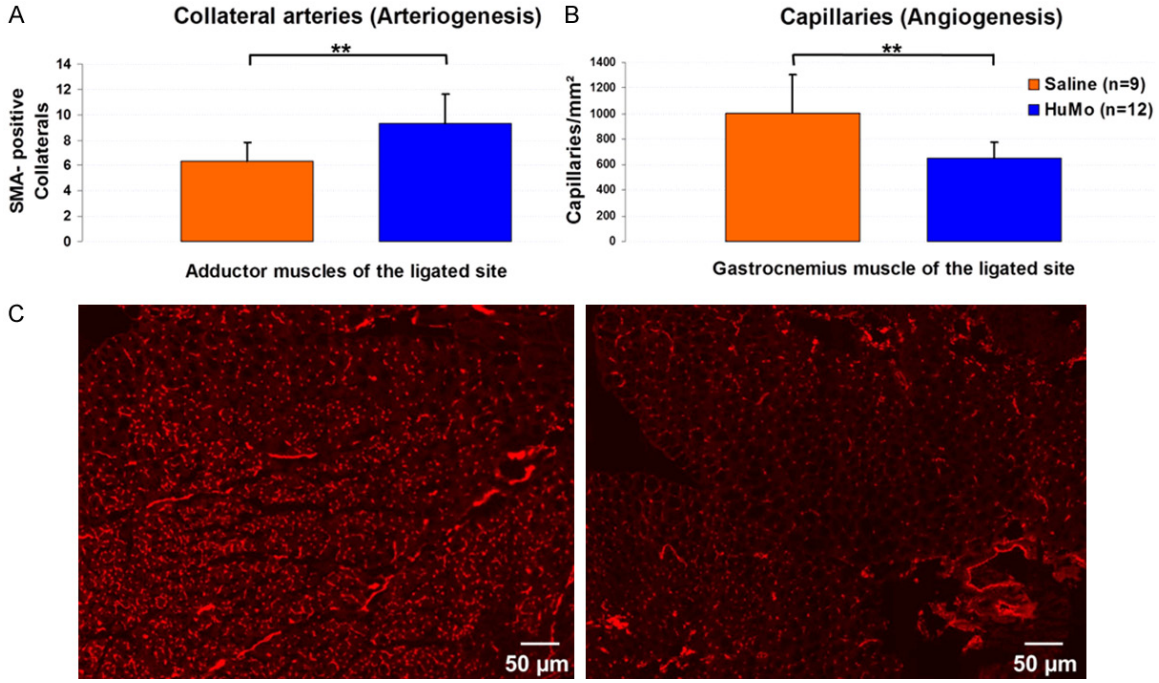

Figure 5. A. Quantification of collateral number within the adductor muscle of the ligated side. B. Quantification of angiogenesis within the lower limb. Comparison of the number of capillaries per mm^2 in the gastrocnemius muscle of the ligated leg 21 days after ligation of the femoral artery. C. Representative immunohistological sections after CD31 staining for capillary density (red) within the gastrocnemius muscle of the ligated leg demonstrate increased ischemia-induced capillary spouting in the control group (left picture) vs. less capillary spouting due to reduced ischemia mediated by increased blood supply by collateral arteries in the proximal musculature in HuMo-treated mice (right picture).

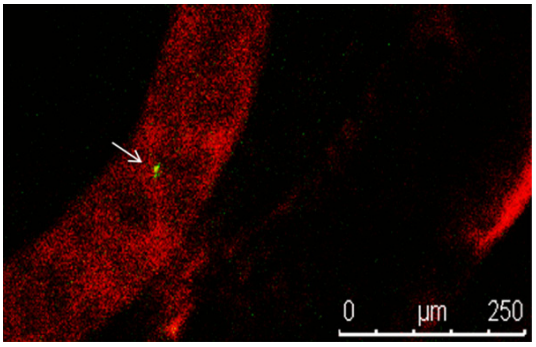

Figure 6. IVM of a vessel at the level of vascular ligation two days after closure of the femoral artery. A labeled monocyte (green (DiO), arrows) within a collateral artery.

tion of new vessel growth within the hind limb (**Figure 7**).

Serum cytokine quantification

Serum was collected prior to and immediately after ligation and at 8 h, 24 h, 72 h, 7 days and

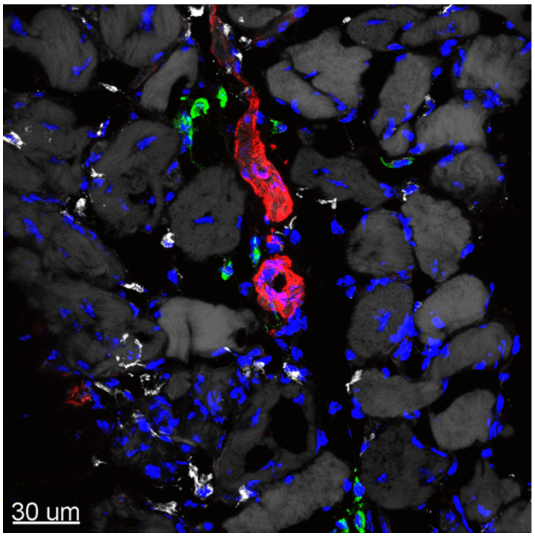

Figure 7. Histological evaluation of the IVM results and visualization of either transplanted HuMo or endogenous mouse Mo. Staining of adductor muscle seven days after systemic monocyte transplantation. Murine monocytes/macrophages = white; human monocyte/macrophages = green, smooth muscle actin = red; nucleus staining DAPI = blue.

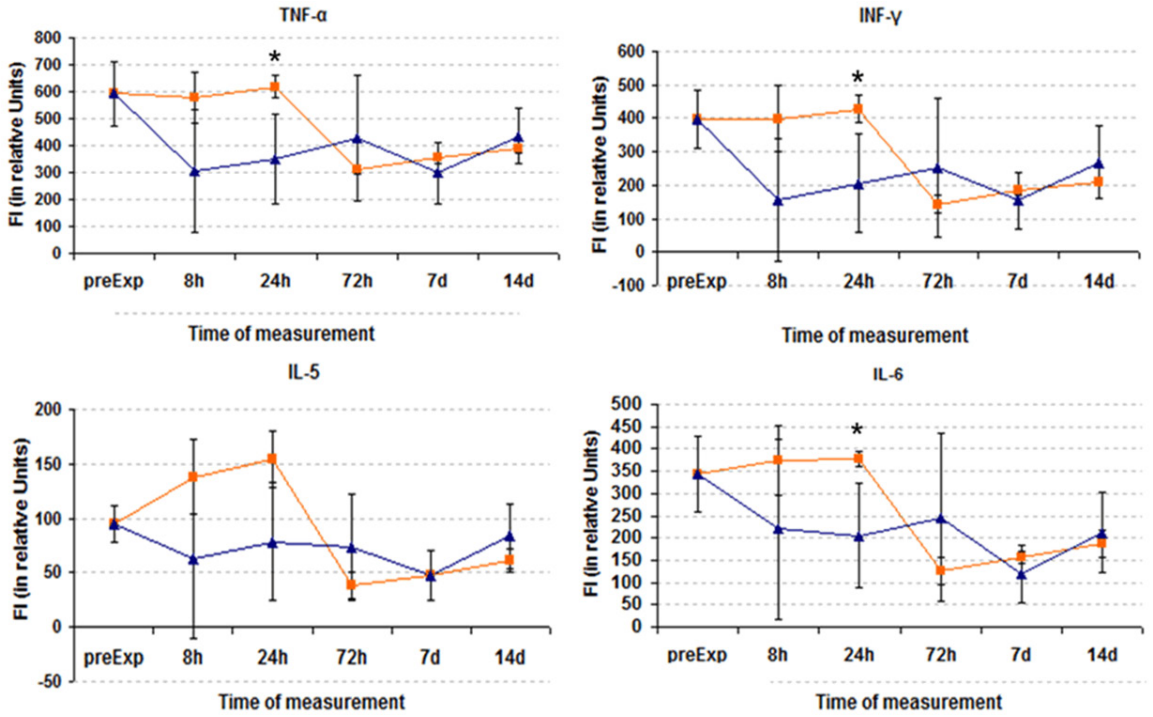

Figure 8. Quantification of cytokines in the serum at different time points. HuMo transplantation group = blue; control saline group = orange.

14 days for cytokine quantification. Significant decreases in TNF-α, INF-Y, IL-4, IL-5, IL-6 and IL-10 were found 8 h after systemic monocyte transplantation (**Figure 8**). All these cytokines had comparable dynamics regarding blood concentration levels 8 h after systemic monocyte transplantation. Although the control and transplant groups began at the same level of deficit following ligation, the physiological process of collateralization after ligation of the femoral artery appeared to be accelerated by xenogenic monocyte transplantation. Interestingly, the same cytokine levels were found after 14 days in both groups.

qRT-PCR

The mRNA expression levels of a proliferation marker (ki67) and cytokine (MCP-1) relevant for leukocyte and monocyte recruitment were studied, and significant differences were not observed in the expression levels of both transcripts in the quadriceps and gastrocnemius muscle of HuMo-treated mice (**Figure 9**).

Discussion

The participation of Mo in the process of arteriogenesis has been demonstrated in several previous studies [11, 12, 14, 27-29]. Because the substitution of single growth factors for improving collateral growth has revealed only minor success [30], our group focuses on the transplantation of Mo. The therapeutic augmentation of collateral vessel growth after the introduction of allogenic, adenoviral-transduced Mo or receptor-engineered Mo has been demonstrated for decades; however, the transfer of these basic research results to human cells has not been previously performed.

We applied Mo during therapeutic cell therapy for PAD (peripheral artery disease) to improve blood perfusion to ischemic areas because of the following reasons: Mo locally secrete all the necessary growth factors at the correct concentrations and at the appropriate time, and in addition to the release of different cytokines, Mo also have the ability to communicate with other cells essential for vascular growth [18, 27, 28]. Therefore, Mo are able to locally promote the complex process of arteriogenesis. The transplantation of murine and rabbit Mo in animal models has successfully increased collateral development [12-14]. To extend this knowledge and take a further step toward the therapeutic use of Mo in humans, experiments

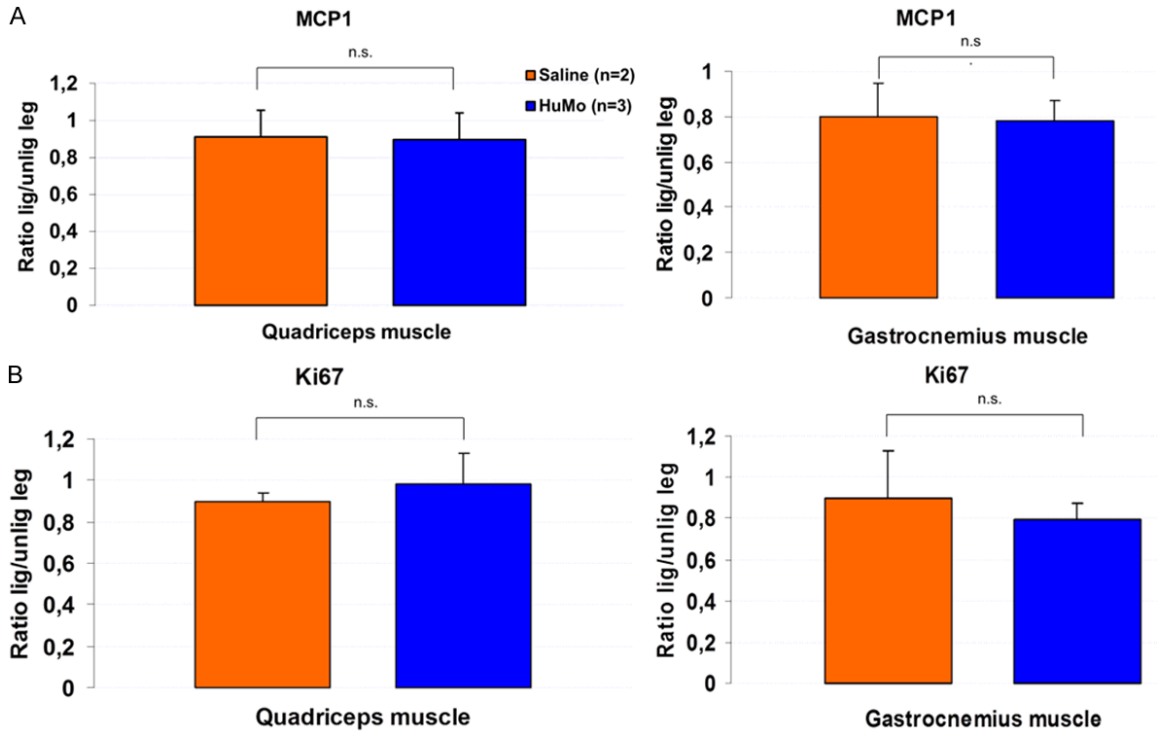

Figure 9. QRT-PCR analyses of MCP-1 and ki67. Bar graphs representing the mRNA expression level of MCP-1 (A) and ki67 (B) in the quadriceps muscle and gastrocnemius muscle of HuMo as well as control mice 3 days after femoral artery ligation. Results were normalized to the expression level of 18 S rRNA. Data are shown as the means ± SD.

with HuMo are necessary, and they must be investigated both *ex vivo* and *in vivo* using animal models. Therefore, in this study, isolated HuMo were systemically transplanted and found to exhibit homing to sites of collateral development. We successfully showed that Mo improved the clinical outcomes after ligature of the femoral artery. To develop future clinical therapeutic approaches, this study focused on stimulating HuMo and subsequent intravenous administration of HuMo in an animal model. In addition to the previously discussed experiments on the effect of Mo transplantation in the development of atherosclerotic plaques, the influence of Mo transplantation on the growth of endogenous tumors must also be examined. Thus, our research group is currently investigating the influence of Mo transplantation on tumor vascularization in a Matrigel-mouse model [31]. Using IVM, the homing of HuMo was demonstrated for the first time after systemic transplantation *in vivo* [16]. The interaction between the transplanted HuMo and endogenous mouse Mo was demonstrated histologically in this study for up to seven days after transplantation for the first time.

Previous studies have demonstrated the success of monocyte research and revealed increased collateral growth in ischemic vascular disease by supporting the lifespan and local concentration of Mo [7, 13, 25, 32]. However, many questions remain that must be clarified prior to clinical application of this promising therapeutic method. The clinically transfer of Mo in humans for the use of therapeutic HuMo transplantation requires further investigation.

For this purpose, HuMo were isolated and the HuMo functional integrity, protein uptake, cell viability, and migration into tissue were tested. Mo were administered to recipient mice via intravenous injection one day after ligation of the femoral artery. The xenogeneic monocyte transplantation led to improved perfusion after 21 days, which was attributed to increased arteriogenesis in the upper limb as demonstrated by an increased number of collaterals and less necrosis.

Our study demonstrated that transplanted HuMo adhere to the vessel wall in the inflammatory environment and migrate into tissue

surrounding growing collateral arteries to promote collateralization. Interactions between exogenic and endogenic Mo were well visualized using immune histochemical techniques. In addition, we showed that these cells were localized around the collateral arteries after 7 days and exhibited perivascular interactions with endogenous, competent murine Mo.

We postulate that a local host vs. graft interaction will lead to the further amplification of inflammation, thus supporting arteriogenesis. This hypothesis of a host vs. graft reaction is supported by the results of Francke et al. [13], who showed that arteriogenesis was inhibited by the administration of cyclosporine A, which specifically targets the signaling pathways in T cells. Collateral generation was predominantly driven by cell interactions of Mo with CD-4 and CD-8 T cells as previously shown by Stabile et al. [28, 33], thus supporting this theory. Stabile et al. found that the absence of CD-4 or CD-8 T cells in knock-out mice did not lead to the sufficient formation of collaterals. However, after transplantation of CD-4 or CD-8 T cells, collaterals could again develop in these mice. In addition, modified syngeneic Mo with an allogeneic character has been successfully used to increase collateral growth. This effect could then be completely inhibited by the depletion of CD-4 T cells [14]. In our experiments to date, we have investigated allogeneic, autologous and syngeneic Mo transplantation in mice and rabbits and achieved promising results in animal experiments [12-14, 17, 34]. Allogeneic cell transplantations are routinely used for the treatment of hematological disease in the form of stem cell transplants. The increased arteriogenesis observed in this study was most likely due to increased activation and recruitment of endogenous Mo.

The results presented here show that human *ex vivo*-stimulated Mo are fully functional and can also lead to changes in vascular growth in living organisms, which are critical findings for the use of this promising therapeutic method in future clinical approaches.

As previously mentioned, the mechanism of xenogeneic monocyte transplantation for the augmentation of collateral vessel growth is poorly understood. Nevertheless the potential of Mo has been previously recognized and enhancement of blood monocyte concentrations and lifespans has been exploited in clinical human studies on the treatment of cad and PAD patients [29, 32].

In this study, monocyte recruitment was not achieved by the administration of systemically infused growth factors but rather by direct transplantation because growth factor-driven studies have indicated that minor clinical results are obtained while considerable side effects occur [35]. Monocytes are non-dividing cells that have no potential to differentiate into other unwanted cell pathways, such as tumor cells.

In this study, we focused on characterizing and confirming the functionality of isolated HuMo for cell transplantation experiments. Successfully demonstrating the isolation, function, transplantation and homing of HuMo can provide a basis for further alternative cell therapies, which are warranted in fighting PAD. Considerably improvements in clinical outcome and restoration of blood supply to ischemic limbs were obtained by this strategy.

The serum cytokine levels in control mice were decreased, particularly in inflammatory cytokines, such as TNF-α, INF-Y and IL-6, starting 48 h after ligation of the femoral artery, which represent the time point when endogenous monocyte transmigration reached a maximum value. Identical slope values were measured when HuMo were transplanted, thus supporting our theory that exogenous Mo transplantation triggers an endogenic shift as well timely as numerous in quantitative Mo, which was confirmed by the robust perivascular infiltration of Mo based on histological analyses and IVM. The average circulating time of Mo in the bloodstream after their release from the bone marrow is between 24 and 72 h [36, 37]. Normally the peak of perivascular endogenous monocyte infiltration around growing collateral arteries occurs by approximately day 3 (72 h post ligation), thus representing Mo-Mo interactions between resident Mo [38, 39] and transmigrated Mo with T cells.

Because inflammatory arteriogenic cytokines increased in the collateral arteries as well as the perivascular tissue, we investigated the mRNA expression level of MCP-1 and the prolif-

eration marker ki67 [9, 40]. Although significant difference were not observed in the upper limb or lower limb, a trend of enhanced proliferation within the quadriceps (upper limb) was observed after HuMo transplantation, which may be related to the mouse strain used in the experiments. BALB/c mice are known to have a lower collateralization capacity than C57-BL-6 mice, which explains the limited difference in the upregulation of the pro-arteriogenic cytokine. Nonetheless, we use the BALB/c mouse because of the necessary therapeutic gap for the better detection of the long-term results of HuMo transplantation on clinical outcomes. Our group has shown that C57BL/6 mice restore blood perfusion within one week after ligation of the femoral artery [41]; therefore, this mouse was not adequate for our set up.

Unfortunately, the concentration of human inflammatory and pro-arteriogenic cytokines produced by the exogenous HuMo was not quantitatively measurable in our setting. Therefore, visualized the postulated mechanism underlying the interaction of HuMo and endogenous inflammatory cells via histochemistry and IVM but failed to quantify this complex mechanism by singular cytokines. Nevertheless, a significant systemic measurement of the timelines of cytokines at up to 14 days facilitates analyses of the possible regulatory pathway.

The results of the experiments performed in this study pave the way for further experiments with HuMo and show that human ex vivo-stimulated Mo are fully functional and can lead to changes in vascular growth in living organisms. This finding is an essential required criterion for the use of this promising therapeutic vehicle cell in pad patients.

The serum cytokine level was assessed to provide a better understanding of the immune response and the mechanism behind this phenomenon; moreover, the cytokine levels in the control group were above those of the HuMo-transplanted group at the time point of maximum collateralization at 72 h post ligation.

The cytokine levels of the two experimental groups were similar three days after monocyte transplantation. This observation is possibly due to the reduced circulation time of the injected Mo. The average circulating time of Mo in the bloodstream after their release from the bone marrow is between 24 and 72 h [36, 37]. Due to the supposed host vs. graft reaction, this circulation time may be shortened after xenogeneic transplantation. This could be due to, for example, increased activity of CD4-positive cells, which leads to faster degradation of the cells [42].

The accelerated migration of injected cells already activated by INF-γ could also occur in the surrounding tissue [24], which was demonstrated by the fact that we detected activated Mo after systemic injection via IVM within 24 h of transplantation in the perivascular tissue [16].

Although the clinical results after HuMo transplantation are clear and lead to an improvement in perfusion and increase in the number of collaterals, it is difficult to explain the mechanism based on a change in cytokine level when xenogenic transplantation was performed. Although it is possible to unequivocally identify the transplantation of HuMo around the collaterals and show their interaction with the endogenous Mo and macrophages morphologically via histology and IVM, the production of pro-arteriogenic cytokines is not detectable via RT-PCR.

Endogenic Mo (termed autologous cells) rather than xenogeneic or allogeneic Mo are the preferred cells for the development of therapeutic approaches in humans. Although not arteriogenic themselves, autologous cells can be modified and engineered *ex vivo* to achieve great potential for improving collateralization as allogeneic and xenogeneic Mo [14].

However, further research is needed before this approach can be applied to humans.

Conclusions

Transplantation of xenogeneic Mo (HuMo) can improve collateral vessel growth and clinical outcomes of mice. These results verify our hypothesis that controlled modulation of the inflammatory mechanism in collateral vessel growth by a local host vs. graft reaction in the hind limbs of ischemic mice could be a novel useful strategy for promoting collateral vessel growth.

Acknowledgements

This work was supported by the ELSE-Kröner-Stiftung, “Promotionskommission” of the Otto-

von-Guericke-University and the DFG (Deutsche Forschungsgemeinschaft, German Research Foundation) SFB 854 (Sonderforschungsbereich, collaborative research center). The authors would like to thank Hans-Holger Gärtner, Audiovisuelles Medienzentrum, Otto-von-Guericke University Magdeburg, Germany, Christine Csapo, Walter Brendel Centre of Experimental Medicine, Munich, Germany, Prof. Dr. rer. nat. Siegfried Kropf for technical and statistical support.

Disclosure of conflict of interest

None.

Address correspondence to: Dr. Joerg Herold, Internal Medicine/Cardiology/Angiology, Max-Ratschow Clinic for Angiology, Grafenstrasse 9, 64283 Darmstadt, Germany. Tel: +49-6151-107 4401; Fax: +49-6151-107 4429; E-mail: joerg_herold@hotmail.com

References

[1] van Royen N, Piek JJ, Schaper W, Fulton WF. A critical review of clinical arteriogenesis research. J Am Coll Cardiol 2010; 55: 17-25.

[2] Sabia PJ, Powers ER, Ragosta M, Sarembock IJ, Burwell LR, Kaul S. An association between collateral blood flow and myocardial viability in patients with recent myocardial infarction. N Engl J Med 1992; 327: 1825-1831.

[3] Meier P, Gloekler S, Zbinden R, Beckh S, de Marchi SF, Zbinden S, Wustmann K, Billinger M, Vogel R, Cook S, Wenaweser P, Togni M, Windecker S, Meier B, Seiler C. Beneficial effect of recruitable collaterals: a 10-year follow-up study in patients with stable coronary artery disease undergoing quantitative collateral measurements. Circulation 2007; 116: 975-983.

[4] Meier P, Hemingway H, Lansky AJ, Knapp G, Pitt B, Seiler C. The impact of the coronary collateral circulation on mortality: a meta-analysis. Eur Heart J 2012; 33: 614-621.

[5] Schaper W, Schaper J. Collateral circulation: heart, brain, kindey, limbs. Boston, MA: Kluwer Academic Publishers; 1993.

[6] Seiler C. The human coronary collateral circulation. Heart 2003; 89: 1352-1357.

[7] Chillo O, Kleinert EC, Lautz T, Lasch M, Pagel JI, Heun Y, Troidl K, Fischer S, Caballero-Martinez A, Mauer A, Kurz ARM, Assmann G, Rehberg M, Kanse SM, Nieswandt B, Walzog B, Reichel CA, Mannell H, Preissner KT, Deindl E. Perivascular mast cells govern shear stress-induced arteriogenesis by orchestrating leukocyte function. Cell Rep 2016; 16: 2197-2207.

[8] Arras M, Mollnau H, Strasser R, Wenz R, Ito WD, Schaper J, Schaper W. The delivery of angiogenic factors to the heart by microsphere therapy. Nat Biotechnol 1998; 16: 159-162.

[9] Wu S, Wu X, Zhu W, Cai WJ, Schaper J, Schaper W. Immunohistochemical study of the growth factors, aFGF, bFGF, PDGF-AB, VEGF-A and its receptor (Flk-1) during arteriogenesis. Mol Cell Biochem 2010; 343: 223-229.

[10] Limbourg A, Korff T, Napp LC, Schaper W, Drexler H, Limbourg FP. Evaluation of postnatal arteriogenesis and angiogenesis in a mouse model of hind-limb ischemia. Nat Protoc 2009; 4: 1737-1746.

[11] Carmeliet P. Mechanisms of angiogenesis and arteriogenesis. Nat Med 2000; 6: 389-395.

[12] Herold J, Pipp F, Fernandez B, Xing Z, Heil M, Tillmanns H, Braun-Dullaeus RC. Transplantation of monocytes: a novel strategy for *in vivo* augmentation of collateral vessel growth. Hum Gene Ther 2004; 15: 1-12.

[13] Francke A, Weinert S, Strasser RH, Braun-Dullaeus RC, Herold J. Transplantation of bone marrow derived monocytes: a novel approach for augmentation of arteriogenesis in a murine model of femoral artery ligation. Am J Transl Res 2013; 5: 155-169.

[14] Herold J, Francke A, Weinert S, Schmeisser A, Hebel K, Schraven B, Roehl FW, Strasser RH, Braun-Dullaeus RC. Tetanus toxoid-pulsed monocyte vaccination for augmentation of collateral vessel growth. J Am Heart Assoc 2014; 3: e000611.

[15] Herold J, Tillmanns H, Xing Z, Strasser RH, Braun-Dullaeus RC. Isolation and transduction of monocytes: promising vehicles for therapeutic arteriogenesis. Langenbecks Arch Surg 2006; 391: 72-82.

[16] Wagner M, Baer C, Zuschratter W, Riek-Burchardt M, Deffge C, Weinert S, Lee JC, Braun-Dullaeus RC, Herold J. Intravital microscopy of monocyte homing and tumor-related angiogenesis in a murine model of peripheral arterial disease. J Vis Exp 2017.

[17] Wagner M, Koester H, Deffge C, Weinert S, Lauf J, Francke A, Lee J, Braun-Dullaeus RC, Herold J. Isolation and intravenous injection of murine bone marrow derived monocytes. J Vis Exp 2014.

[18] Weinert S, Poitz DM, Auffermann-Gretzinger S, Eger L, Herold J, Medunjanin S, Schmeisser A, Strasser RH, Braun-Dullaeus RC. The lysosomal transfer of LDL/cholesterol from macrophages into vascular smooth muscle cells induces their phenotypic alteration. Cardiovasc Res 2013; 97: 544-552.

[19] Berthold F. Isolation of human monocytes by ficoll density gradient centrifugation. Blut 1981; 43: 367-371.

[20] Menck K, Behme D, Pantke M, Reiling N, Binder C, Pukrop T, Klemm F. Isolation of human monocytes by double gradient centrifugation and their differentiation to macrophages

in teflon-coated cell culture bags. J Vis Exp 2014; e51554.
[21] Herold J, Nowak S, Kostin S, Daniel JM, Francke A, Subramaniam S, Braun-Dullaeus RC, Kanse SM. Factor VII activating protease (FSAP) influences vascular remodeling in the mouse hind limb ischemia model. Am J Transl Res 2017; 9: 3084-3095.
[22] Wuestenfeld JC, Herold J, Niese U, Kappert U, Schmeisser A, Strasser RH, Braun-Dullaeus RC. Indocyanine green angiography: a new method to quantify collateral flow in mice. J Vasc Surg 2008; 48: 1315-1321.
[23] Scholz D, Ito W, Fleming I, Deindl E, Sauer A, Wiesnet M, Busse R, Schaper J, Schaper W. Ultrastructure and molecular histology of rabbit hindlimb collateral artery growth (arteriogenesis). Virchows Arch 2000; 436: 257-270.
[24] Chomczynski P, Sacchi N. Single-step method of RNA isolation by acid guanidinium thiocyanate-phenol-chloroform extraction. Anal Biochem 1987; 162: 156-159.
[25] Francke A, Herold J, Weinert S, Strasser RH, Braun-Dullaeus RC. Generation of mature murine monocytes from heterogeneous bone marrow and description of their properties. J Histochem Cytochem 2011; 59: 813-825.
[26] Yao Q, Doan LX, Zhang R, Bharadwaj U, Li M, Chen C. Thymosin-alpha1 modulates dendritic cell differentiation and functional maturation from human peripheral blood CD14+ monocytes. Immunol Lett 2007; 110: 110-120.
[27] Hoefer IE, Grundmann S, van Royen N, Voskuil M, Schirmer SH, Ulusans S, Bode C, Buschmann IR, Piek JJ. Leukocyte subpopulations and arteriogenesis: specific role of monocytes, lymphocytes and granulocytes. Atherosclerosis 2005; 181: 285-293.
[28] Stabile E, Burnett MS, Watkins C, Kinnaird T, Bachis A, La Sala A, Miller JM, Shou M, Epstein SE, Fuchs S. Impaired arteriogenic response to acute hindlimb ischemia in CD4-knockout mice. Circulation 2003; 108: 205-210.
[29] van Royen N, Schirmer SH, Atasever B, Behrens CYH, Ubbink D, Buschmann EE, Voskuil M, Bot P, Hoefer I, Schlingemann RO, Biemond BJ, Tijssen JG, Bode C, Schaper W, Oskam J, Legemate DA, Piek JJ, Buschmann I. START trial: a pilot study on STimulation of ARTeriogenesis using subcutaneous application of granulocyte-macrophage colony-stimulating factor as a new treatment for peripheral vascular disease. Circulation 2005; 112: 1040-1046.
[30] van Royen N, Piek JJ, Legemate DA, Schaper W, Oskam J, Atasever B, Voskuil M, Ubbink D, Schirmer SH, Buschmann I, Bode C, Buschmann EE. Design of the START-trial: STimulation of ARTeriogenesis using subcutaneous application of GM-CSF as a new treatment for peripheral vascular disease. A randomized, double-blind, placebo-controlled trial. Vasc Med 2003; 8: 191-196.
[31] Albini A, Melchiori A, Garofalo A, Noonan DM, Basolo F, Taraboletti G, Chader GJ, Gavazzi R. Matrigel promotes retinoblastoma cell growth *in vitro* and *in vivo*. Int J Cancer 1992; 52: 234-240.
[32] Buschmann IR, Hoefer IE, van Royen N, Katzer E, Braun-Dulleaus R, Heil M, Kostin S, Bode C, Schaper W. GM-CSF: a strong arteriogenic factor acting by amplification of monocyte function. Atherosclerosis 2001; 159: 343-356.
[33] Stabile E, Kinnaird T, la Sala A, Hanson SK, Watkins C, Campia U, Shou M, Zbinden S, Fuchs S, Kornfeld H, Epstein SE, Burnett MS. CD8+ T lymphocytes regulate the arteriogenic response to ischemia by infiltrating the site of collateral vessel development and recruiting CD4+ mononuclear cells through the expression of interleukin-16. Circulation 2006; 113: 118-124.
[34] Herold J, Brucks S, Boenigk H, Said SM, Braun-Dullaeus RC. Ultrasound guided thrombin injection of pseudoaneurysm of the radial artery after percutaneous coronary intervention. Vasa 2011; 40: 78-81.
[35] Isner JM, Ropper A, Hirst K. VEGF gene transfer for diabetic neuropathy. Hum Gene Ther 2001; 12: 1593-1594.
[36] van Furth R, Cohn ZA. The origin and kinetics of mononuclear phagocytes. J Exp Med 1968; 128: 415-435.
[37] Whitelaw DM. The intravascular lifespan of monocytes. Blood 1966; 28: 455-464.
[38] Khmelewski E, Becker A, Meinertz T, Ito WD. Tissue resident cells play a dominant role in arteriogenesis and concomitant macrophage accumulation. Circ Res 2004; 95: E56-E64.
[39] Ito WD, Khmelevski E. Tissue macrophages: "satellite cells" for growing collateral vessels? A hypothesis. Endothelium 2003; 10: 233-235.
[40] Buschmann I, Heil M, Jost M, Schaper W. Influence of inflammatory cytokines on arteriogenesis. Microcirculation 2003; 10: 371-379.
[41] Helisch A, Wagner S, Khan N, Drinane M, Wolfram S, Heil M, Ziegelhoeffer T, Brandt U, Pearlman JD, Swartz HM, Schaper W. Impact of mouse strain differences in innate hindlimb collateral vasculature. Arterioscler Thromb Vasc Biol 2006; 26: 520-526.
[42] Swijnenburg RJ, Schrepfer S, Govaert JA, Cao F, Ransohoff K, Sheikh AY, Haddad M, Connolly AJ, Davis MM, Robbins RC, Wu JC. Immunosuppressive therapy mitigates immunological rejection of human embryonic stem cell xenografts. Proc Natl Acad Sci U S A 2008; 105: 12991-12996.